Macromolecules

Article

pubs.acs.org/Macromolecules

Pressure Effects on the Dynamic Heterogeneity of Miscible Poly(vinyl acetate)/Poly(ethylene oxide) Blends

George Zardalidis and George Floudas*

Department of Physics, University of Ioannina, P.O. Box 1186, GR-45110 Ioannina, Greece, and Foundation for Research and Technology-Hellas (FORTH), Biomedical Research Institute (BRI), Ioannina, Greece

Supporting Information

ABSTRACT: The poly(vinyl acetate) (PVAc) segmental dynamics is studied as a function of composition, temperature, and pressure in thermodynamically miscible blends with poly(ethylene oxide) (PEO) by dielectric spectroscopy. In the PVAc-rich blends all short-range correlations are dominated by the PVAc component. An invariant frequency dispersion is found when the spectra at each blend composition are compared under isochronal conditions. The self-concentration model with a fixed PVAc self-concentration of ∼0.22 qualitatively describes the temperature dependence of the PVAc segmental dynamics both at atmospheric and at elevated pressures.

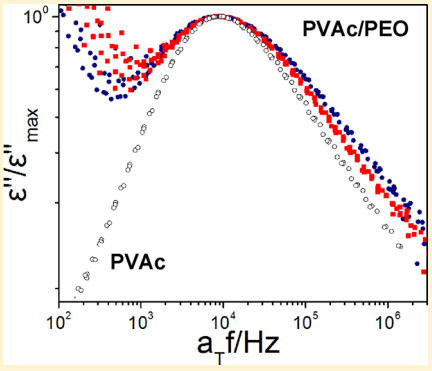

INTRODUCTION

Understanding component segmental dynamics in miscible polymer blends has been a key issue in polymer dynamics and in the physics of polymers, in general. In particular, the term "dynamic heterogeneity" refers to the presence of distinct segmental dynamics in thermodynamically mixed blends.[1−7] This dynamic heterogeneity has as specific signatures the broadening of the relaxation spectra with respect to the homopolymers and the dual relaxation processes that reflect the component segmental dynamics. From a theoretical point of view, approaches that are based on the coupling model,[2,8] concentration fluctuations,[9] chain connectivity[10] or combination of both[11−18] have considered in explaining the experimental features of dynamic heterogeneity. In particular, the model of thermally driven concentration fluctuations[9] was successful in explaining the broadening of relaxation spectra whereas the model that emphasizes the effect of chain connectivity[10] on the local effective concentration provides with direct predictions for the component dynamics that can readily be tested experimentally.

According to the self-concentration model of Lodge and McLeish (LM),[10] chain connectivity enhances the local concentration, and as a result the segmental dynamics of a given polymer are biased to those of the corresponding homopolymer. The relevant length scale for evaluating the self-concentration is the Kuhn length that should only moderately depend on temperature and pressure. Although the model predictions have been tested against "isobaric" experiments made at atmospheric pressure, very little is known on how increasing pressure affects the relaxation times within the LM model. Dielectric spectroscopy (DS) is a versatile experimental tool in studying component segmental dynamics as a function of temperature and pressure.[19−28] In a recent study,[29] the poly(methyl methacrylate) (PMMA) segmental dynamics were investigated as a function of pressure in miscible blends with poly(ethylene oxide) (PEO). It was shown that the model predictions can account for the composition dependence of the PMMA glass temperature. However, the strong dielectric activity of the PMMA β-process precluded a detailed test of the model against the full $\tau(P)$ dependence of relaxation times.

A miscible blend where the slow segmental process has a strong dielectric activity (and a weaker β-process) and at the same time the blend possess significant dynamic asymmetry (i.e., difference in glass temperatures, ΔT_g) is the poly(vinyl acetate)/PEO with a $\Delta T_g \sim 100$ K. PVAc/PEO blends have been investigated earlier with respect to the thermodynamic state,[30,31] the PEO crystallization behavior,[32,33] the PEO segmental and terminal dynamics,[34,35] and the PVAc segmental dynamics at atmospheric pressure.[33,34,36,37] Very different segmental dynamics for the two components were found in accord with the LM model. However, in these experiments[33,34,36,37] the PVAc self-concentration varied by a factor of 3 (from 0.23 to 0.08). It is the purpose of the present investigation to test the LM model predictions for the PVAc segmental dynamics both at atmospheric and at elevated pressures. For this purpose, the model is extended to account for pressure effects.

Blends of PVAc/PEO have a negative energy of mixing suggesting miscibility.[31] The system exhibits a LCST behavior and a very asymmetric phase diagram.[30,31] With increasing

Received: May 29, 2012
Revised: July 5, 2012
Published: July 23, 2012

dx.doi.org/10.1021/ma301086a | Macromolecules 2012, 45, 6272−6280

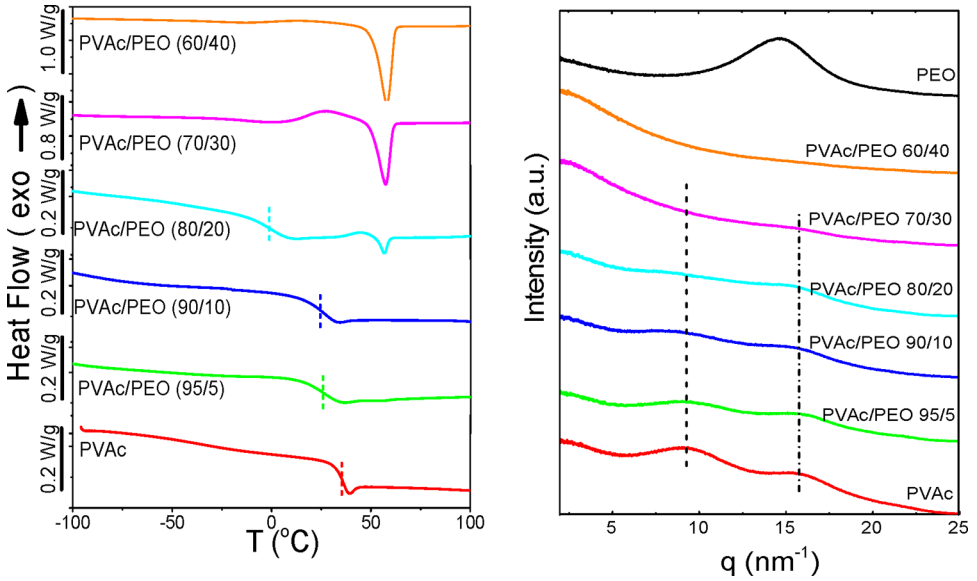

Figure 1. (left) DSC thermograms of the PVAc homopolymer and the blends rich in PVAc. The vertical dashed lines indicate the glass temperatures extracted by DSC. (right) WAXS from the same blends obtained at 353 K. The vertical lines give the positions of the PVAc peaks in the blends.

PVAc molecular weight, the phase boundaries shift toward lower temperatures and the critical composition shifts toward higher PEO concentration. The negative mixing enthalpy is the result of specific interactions between the two components. Different specific interactions have been considered: (i) hydrogen bonds between the oxygen atom of PEO and one hydrogen from the PVAc methyl group and (ii) dipole−dipole interactions between the negatively charged oxygen in PEO and the positively charged PVAc carbonyl carbon. As pressure can affect both types of interactions, it is of interest to explore the PVAc dynamics in the PVAc/PEO blends.

EXPERIMENTAL SECTION

Samples. The PEO (M_w = 32 500 g/mol, M_w/M_n = 1.09) and PVAc (M_w = 59 400 g/mol, M_w/M_n = 2.8) used in this study were purchased from Polymer Source Inc. Blends with 5, 10, 20, 30, and 40 wt % PEO were prepared from chloroform solutions. The solutions were stirred for several hours and then dried for ∼24 h under vacuum to remove any remaining solvent. Subsequently, the samples were heated to 373 K and sandwiched between two brass electrodes to form a capacitor.

Differential Scanning Calorimetry (DSC). The thermal behavior was determined by differential scanning calorimetry on cooling and subsequent heating at a rate of 10 K/min with a Mettler 30 DSC under a N_2 atmosphere. The DSC traces from the second heating scan of the homopolymers and the corresponding blends are compared at 353 K shown in Figure 1.

X-ray Scattering. Wide-angle X-ray scattering (WAXS) measurements have been performed from extruded fibers at 298 K using a pinhole collimator and a mar345 image plate detector system (plate diameter 345 mm, pixel size 150 μm^2). A graphite monochromator was used (λ = 0.154 nm), and the sample-to-detector distance was 23 cm. Measurements of 1 h long were made within the temperature range from 303 to 353 K on heating and on subsequent cooling in steps of 10 K. The recorded 2-D scattered intensities were investigated over the azimuthal angle and are presented as a function of the scattering wave vector q ($q = (4\pi/\lambda)\sin(2\theta/2)$, where 2θ is the scattering angle). Figure 1 compares the WAXS integrated intensities at 353 K.

Dielectric Spectroscopy (DS). Dielectric measurements were made with a Novocontrol Alpha frequency analyzer under "isobaric" conditions as a function of temperature and under "isothermal" conditions as a function of pressure. The "isobaric" measurements were performed at different temperatures in the range 173.15−423.15 K in steps of 2 or 5 K, at atmospheric pressure, and for frequencies in the range from 10^{-2} to 10^7 Hz. The sample capacitor had a diameter of 20 mm while the thickness was maintained with the use of Teflon spacers at 50 μm. The "isothermal" measurements were carried out with a Novocontrol BDS system, comprising a frequency response analyzer (Solartron Schlumberger FRA 1260) and a broadband dielectric converter with an active sample head, in the range from 10^{-2} to 3×10^6 Hz. Measurements under hydrostatic pressure were carried out in a Novocontrol pressure cell.[20] The pressure setup consists of a temperature controlled cell, hydraulic closing press with air pump, and air pump for hydrostatic test pressure. The sample capacitor was composed of two 20 mm diameter electrodes wrapped with a Teflon tape and placed inside a Teflon ring, in order to prevent oil leakage inside the sample volume. The sample was submerged in a silicon oil filled vessel where the pressure was increased and measurements were taken up to 240 MPa in steps of 20 MPa, while keeping the temperature constant at values of 333, 343, 353, 363, 373, and 383 K. To prevent electrode contact at high pressures, the thickness of the samples was maintained with the use of Teflon spacers at 100 μm. The "isothermal" frequency sweeps were made with a temperature stability better than ±0.1 K and a pressure stability better than ±2 MPa. In every case the complex dielectric permittivity $\varepsilon^* = \varepsilon' - i\varepsilon''$, where ε' is the real and ε'' is the imaginary part, was obtained as a function of frequency ω, temperature T, and pressure P, i.e., $\varepsilon^*(T,P,\omega)$. The analysis of both T- and P-dependent experiments was made using the empirical equation of Havriliak and Negami (HN):[38,39]

$$\varepsilon^*(T, P, \omega) = \varepsilon_\infty(T, P) + \frac{\Delta\varepsilon(T, P)}{[1 + (i\omega\tau_{HN}(T, P))^m]^n} + \frac{\sigma_0(T, P)}{i\varepsilon_f\omega} \quad (1)$$

where $\varepsilon_\infty(T,P)$ is the high-frequency permittivity, $\tau_{HN}(T,P)$ is the characteristic relaxation time in this equation, $\Delta\varepsilon(T,P) = \varepsilon_0(T,P) - \varepsilon_\infty(T,P)$ is the relaxation strength, m, n (with limits $0 < m$, $mn \leq 1$) describe respectively the symmetrical and asymmetrical broadening of the distribution of relaxation times, σ_0 is the dc conductivity, and ε_f is the permittivity of free space. From τ_{HN}, the relaxation time at maximum loss, τ_{max}, is obtained analytically following

dx.doi.org/10.1021/ma301086a | Macromolecules 2012, 45, 6272−6280

$$\tau_{max} = \tau_{HN}\left[\frac{\sin\left(\frac{\pi m}{2+2n}\right)}{\sin\left(\frac{\pi mn}{2+2n}\right)}\right]^{-1/m} \quad (2)$$

At lower frequencies, ε'' rises due to the conductivity ($\varepsilon'' = \sigma/(\omega\varepsilon_f)$). The measured ε'' spectra have been used for the analysis except at high temperatures where the derivative of ε' has been employed ($d\varepsilon'/d \ln \omega \sim -(2/\pi)\varepsilon''$). This method is useful in fitting relaxation processes which are hidden under the conductivity, provided that the system is free of surface polarization effects.

RESULTS AND DISCUSSION

Miscibility. Figure 1 gives the DSC traces of the PVAc/PEO blends rich in PVAc and the corresponding wide-angle scattering curves at 353 K. The main characteristics of the DSC curves are the reduced PVAc glass temperatures and the onset of PEO crystallization already at $\varphi_{PVAc} = 0.8$. The extracted degree of PEO crystallinity ($X_c = \Delta H/w_{PEO}\Delta H_0$, where ΔH is the measured heat of fusion and ΔH_0 is the heat of fusion for a 100% crystalline PEO) amounts to 3%, 49%, and 67% for the blends with $\varphi_{PVAc} = 0.8$, 0.7, and 0.6, respectively. Clearly, in the blends with $\varphi_{PVAc} = 0.7$ and 0.6 there is phase separation.

Additional information on the thermodynamic state of the mixtures can be extracted from X-ray scattering. The scattering curves of the homopolymers are compared with the PVAc-rich blends in Figure 1 at 353 K, that is, above the PEO melting point. The PVAc scattering curve contains two maxima within the investigated q-range (at $q \sim 9.2$ and 16.2 nm^{-1}). The distances can be calculated from $d = 2\pi z/q$, where $z = 1.23$ accounts for nearest-neighbor correlations only.[40] The corresponding distances at 0.477 and 0.835 nm reflect van der Waals nearest-neighbor correlations and longer-range correlations, respectively. In PEO, a single maximum is obtained corresponding to an intermediate distance of 0.53 nm. In the blends with $\varphi_{PVAc} = 0.95$, 0.9, and 0.8, all short-range correlations are dominated by PVAc. On the contrary, in the blends with $\varphi_{PVAc} = 0.7$ and 0.6 these correlations are not the dominant as additional scattering appears at lower angles. This excess scattering suggests phase separation already in the melt state and explains the origin of PEO crystallization in blends with $\varphi_{PVAc} = 0.7$ and 0.6. These results are consistent with earlier thermodynamic data that suggested a LCST behavior with a very asymmetric phase diagram with a critical composition shifted toward the PEO component.[31] On the other hand, in the blend with $\varphi_{PVAc} = 0.8$, the scattering at low angles is not as strong suggesting partial miscibility. On the basis of the above, we restrict our investigation of dynamic heterogeneity in the thermodynamically miscible blends with $\varphi_{PVAc} = 0.95$, 0.9, and 0.8.

Segmental Dynamics as a Function of Temperature. The segmental dynamics in the PVAc homopolymer and the three blends were investigated by DS. Figure 2 provides some representative fits of the dielectric loss curves with the HN function including the conductivity contribution at lower frequencies. In these curves one can notice an increasing contribution from ionic conductivity with increasing PEO fraction. This suggests that PEO promotes ionic (impurity) transport as has been observed in several PEO/electrolyte systems.[41] On the other hand, this feature precludes the analysis of the PEO segmental dynamics in the PVAc/PEO blends. Therefore, in the remaining we restrict our study to the PVAc segmental dynamics in the PVAc-rich blends.

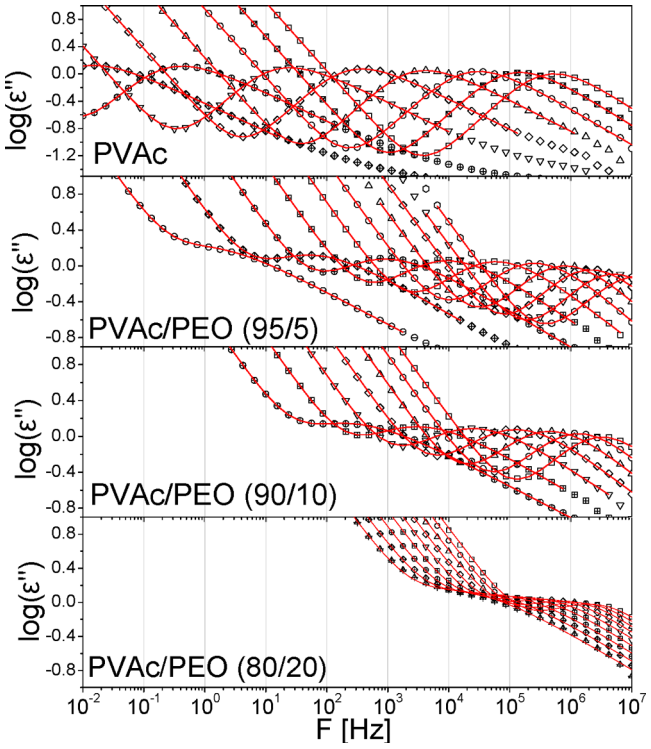

Figure 2. Dielectric loss curves for PVAc and the blends at different temperatures at 0.1 MPa. The PVAc data are within the T-range from 313.15 to 378.15 K, the PVAc/PEO 95/5 blend within the T-range from 318.15 to 408.15 K, the PVAc/PEO 90/10 blend within the T-range from 328.15 to 388.15 K, and the PVAc/PEO 80/20 blend within the T-range from 333.15 to 373.15 K. Lines are fits to a single HN function with a conductivity contribution at lower frequencies.

Figure 3 gives the T-dependence of the low (m) and high (n) frequency slopes of the PVAc segmental dynamics in the blends at 0.1 MPa. The PVAc segmental process has a narrow distribution of relaxation times ($m \sim 0.9$) with a temperature-dependent high-frequency slope varying from 0.41 to 0.71. This

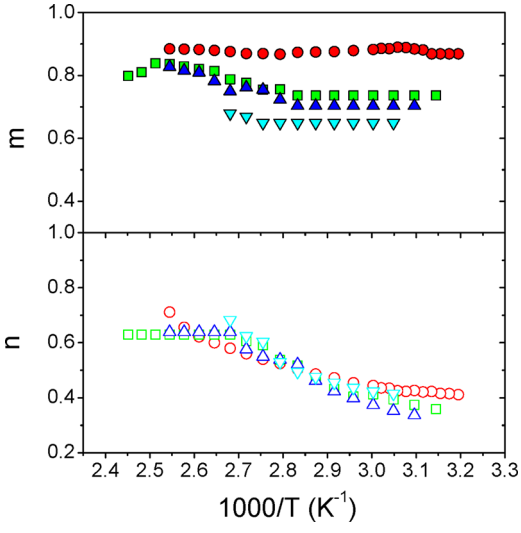

Figure 3. Temperature dependence of the low (m, filled symbols)) and high (n, open symbols) frequency HN parameters of the PVAc segmental process in the homopolymer and in the blends: PVAc (circles), PVAc/PEO blends with $\varphi_{PVAc} = 0.95$ (squares), $\varphi_{PVAc} = 0.90$ (up triangles), and $\varphi_{PVAc} = 0.80$ (down triangles).

dx.doi.org/10.1021/ma301086a | Macromolecules 2012, 45, 6272−6280

T-dependence results in the breakdown of time−temperature superposition (tTs) for bulk PVAc. We speculate that increasing temperature changes the existing specific interactions even in bulk PVAc, and this shows up in the effective dielectric strength ($T\Delta\varepsilon$) that is now strongly T-dependent (Figure S1, Supporting Information). In the blends, the low-frequency slope changes systematically with composition, suggesting a broadening in the distribution of relaxation times. This feature has been discussed before with respect to concentration fluctuations.[9] Figure 4 gives the respective relaxation times

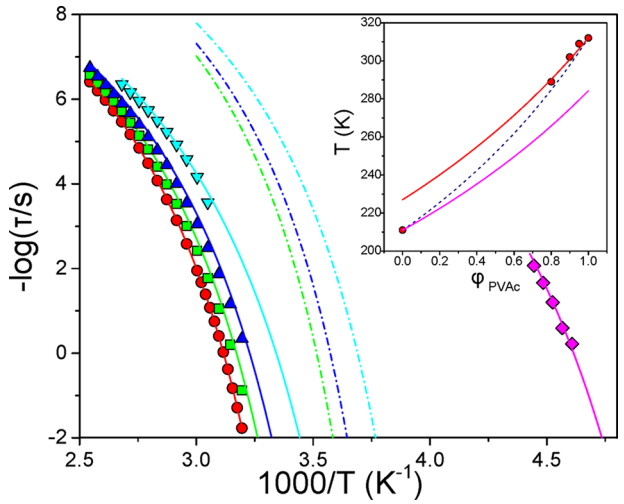

Figure 4. Segmental relaxation times at P = 0.1 MPa for the bulk PVAc (circles), bulk PEO (rhombi), and the slow component in the PVAc/PEO blends with φ_{PVAc} = 0.95 (squares), φ_{PVAc} = 0.90 (up triangles), and φ_{PVAc} = 0.80 (down triangles). The solid lines for the homopolymers represent fits to the VFT equation, whereas in the blends the solid lines give the predictions of the LM model using l_k = 1.36 nm for the Kuhn length and a self-concentration of 0.22. The dash-dotted lines are the LM model predictions for the respective PEO dynamics in the same blends (same color code). In the inset the glass temperatures, obtained from DS at τ = 100 s, are plotted as a function of φ_{PVAc} at 0.1 MPa. The dashed line is the Fox equation whereas the red and magenta solid lines are the LM model predictions for the PVAc (φ_S = 0.22) and PEO (φ_S = 0.21) glass temperatures in the blends without any adjustable parameters.

for the PVAc and the three blends. The $\tau(T)$ dependence conforms to the Vogel−Fulcher−Tammann (VFT) equation

$$\tau = \tau_0 \exp\left(\frac{B}{T - T_0}\right) \tag{3}$$

where τ_0 is the relaxation time in the limit of very high temperatures, B is the activation parameter, and T_0 is the "ideal" glass temperature (Table 1). The lines for the homopolymer $\tau(T)$ represent the result of the fits to eq 3 whereas in the blends the lines are model predictions (see below).

Comparison with the Self-Concentration Model. Earlier[42] (and the current) measurements of the PVAc segmental dynamics as a function of temperature and pressure revealed that the molecular dynamics reflect mainly intramolecular effects. It is thus natural to employ the "self-concentration" model of Lodge and McLeish (LM) that is based on intramolecular effects and nondiverging length scales. According to the model,[10] the average composition of the local environment around any chosen segment is enriched in the

Table 1. Parameters of the VFT Equation at P = 0.1 MPa for the Bulk PVAc and the Blends

	−log(τ_0/s)	B (K)	T_0 (K)
PVAc	11.85 ± 0.03	1663 ± 11	260.0 ± 0.2
PVAc/PEO (95/5)	11.7 ± 0.1	1632 ± 45	256.5 ± 1.2
PVAc/PEO (90/10)	11.5 ± 0.1	1529 ± 53	254.2 ± 1.6
PVAc/PEO (80/20)	11.5[a]	1627 ± 24	236.0 ± 1.6

[a]Held fixed.

same species because of chain connectivity effects (correlation hole effect). The effective local concentration is defined by

$$\varphi_{\mathrm{eff},i} = \varphi_{S,i} + (1 - \varphi_{S,i})\langle\varphi\rangle \tag{4}$$

Here i represents component A or B, φ_S is the self-concentration, and $\langle\varphi\rangle$ is the average blend composition. We note that lattice model calculations[18] results in a self-consistent definition of φ_{eff} (in the present case though—see below—there are only minor differences). According to the LM model, the relevant length scale in evaluating the self-concentration is the Kuhn length (l_K) of the polymer. The self-concentration is determined from the volume fraction occupied by monomers in one Kuhn length inside a volume $V = l_K^3$ as

$$\varphi_S = \frac{C_\infty M_0}{k\rho N_A V_K} \tag{5}$$

where C_∞ is the characteristic ratio, M_0 is the repeated unit molar mass, N_A is the Avogadro number, ρ is the density, and k is the number of backbone bonds per repeat unit. The model associates the average local concentration φ_{eff} for each component with a local glass temperature as $T_{g,eff} = T_g(\varphi)|_{\varphi=\varphi_{eff}}$. For the macroscopic composition dependence of the glass temperature the Fox equation is assumed as

$$\frac{1}{T_g(\varphi_{eff})} = \frac{\varphi_{eff}}{T_g^A} + \frac{1 - \varphi_{eff}}{T_g^B} \tag{6}$$

The full $\tau(T)$ dependence of the component dynamics in the blends can be predicted by further assuming the VFT equation with identical B_i and $\tau_{0,i}$ parameters as for the respective homopolymers and that only the ideal glass temperature varies with composition as

$$T_{0,i}(\varphi_{eff}) = T_{0,i} + [T_{g,i}(\varphi_{eff}) - T_{g,i}] \tag{7}$$

where $T_{0,i}$ is the ideal glass temperature for homopolymers A or B and $T_{0,i}(\varphi_{eff})$ is the ideal glass temperature for each component in the blends.

These predictions are tested for the PVAc dynamics in the three blends in Figure 4 at 0.1 MPa using C_∞ = 8.79,[43] M_0 = 0.0861 kg/mol, k = 2, ρ = 1190 kg/m^3, l_K = 1.36 nm resulting in φ_S = 0.22 for PVAc and C_∞ = 5.5,[44] M_0 = 0.044 kg/mol, k = 3, ρ = 1212 kg/m^3, l_K = 0.81 nm resulting in φ_S = 0.21 for PEO. There is a qualitative agreement of the $\tau(T)$ dependence with the LM model predictions for the PVAc segmental dynamics in the blends with φ_{PVAc} = 0.95 and 0.9, whereas for φ_{PVAc} = 0.80 the agreement is nearly quantitative. We mention here that the theoretical lines have no adjustable parameters. As expected, the model correctly captures the $T_g(\varphi_{PVAc})$ dependence at 0.1 MPa shown in the inset to Figure 4. On the other hand, the model predictions for the PEO segmental relaxation in the same blends (dashed lines) could not be tested against experimental data for reasons discussed earlier.

dx.doi.org/10.1021/ma301086a | Macromolecules 2012, 45, 6272−6280

Segmental Dynamics as a Function of Pressure. Investigating the segmental dynamics as a function of pressure has two advantages: (i) it can unambiguously provide the origin of the dynamic processes (through the pressure sensitivity of the relaxation times and the pressure coefficient of the respective glass temperature) and (ii) provides the possibility to test the LM model predictions at elevated pressures. The PVAc segmental dynamics in the blends were subsequently investigated as a function of pressure.

Before we discuss the detailed $\tau(P)$ dependence, we first discuss the result of the attempted temperature−pressure superposition (TPs) of the PVAc segmental dynamics in bulk PVAc and in two blends with respect to Figure 5. The dielectric loss data for each system are superimposed by employing spectra at different temperatures and pressures, all resulting at "isochronal" peak positions. In the data we have applied only small horizontal shifts (i.e., $a_T \sim 1$) to account for the experimental T, P conditions. Despite the temperature-dependent widths of the distributions for each of the components at atmospheric pressure, when compared under isochronal conditions, the data result in a perfect superposition. This feature, of an invariant frequency dispersion of the α-process at constant relaxation time for spectra taken under different combinations of T and P, is a remarkable feature of the dynamics in glass-forming liquids, amorphous polymers, and polymer blends.[45] The coupling model for polymer blends is the only theoretical approach that has a prediction consistent with this experimental finding, in that a constant dispersion width is the prerequisite to maintain a constant structural relaxation time.[46,19]

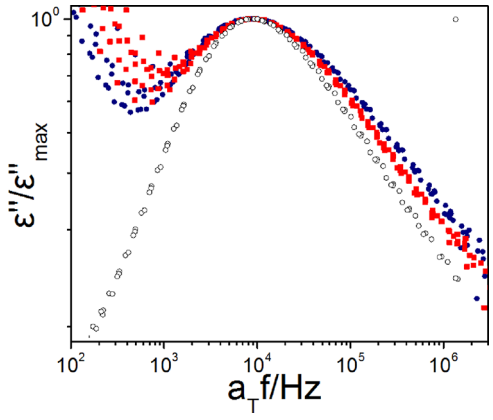

Figure 5. Temperature and pressure superpositions of the normalized dielectric loss of PVAc (open circles) and PVAc/PEO blends with $\varphi_{PVAc} = 0.95$ (squares) and $\varphi_{PVAc} = 0.90$ (filled circles) corresponding to nearly the same peak frequency (i.e., horizontal shift factor, $a_T \sim 1$). Notice the good spectral superposition despite the very different T and P conditions.

Figure 6 gives the corresponding "isobaric" and "isothermal" representations of the segmental relaxation times. The latter were described by the pressure counterpart of the temperature VFT equation[47]

$$\tau = \tau_0 \exp\left(\frac{CP}{P_0 - P}\right) \tag{8}$$

The apparent activation volume, $\Delta V^{\#}$, defined as

$$\Delta V^{\#} = RT\left(\frac{\partial \ln \tau}{\partial P}\right)_T \tag{9}$$

when applied to the nonlinear $\tau(P)$ dependence (Figure 7) increase in a nonlinear fashion as predicted by eqs 8 and 9 as

$$\Delta V^{\#} = RT\frac{CP_0}{(P_0 - P)^2} \tag{10}$$

The activation volume is a very useful parameter to characterize the relaxation processes in glass-forming liquids. In the framework of the transition state theory, the apparent activation volume, $\Delta V^{\#}$, is defined as the difference between the volumes occupied by a molecule in activated (transition) and nonactivated (minimum) states. Thus, the value of $\Delta V^{\#}$ may reflect on the volume requirements for local molecular motion. This has been explored in a number of polymers and other glass-forming liquids.[19] It has been shown[48,49] that $\Delta V^{\#}$ (i) scales with the temperature difference from T_g for homopolymers of different molecular weights, (ii) shows a strong T-dependence especially in the vicinity of T_g, and (iii) approaches the monomer volume for temperatures in the range 70−90 K above T_g. The distinctly different pressure sensitivity of the segmental relaxation times of different polymers possessing different monomer units has been employed as a fingerprint of the heterogeneous dynamics in miscible[21] or weakly phase separated polymer blends.[23]

This notion is tested in Figure 8 where the apparent activation volume of the PVAc segmental process in the PVAc-rich blends is plotted at temperatures equidistant from the respective glass temperatures, at $P = 0.1$ MPa (a comparison over different pressures is made in Figure S2, Supporting Information). It can be seen that (i) the apparent activation volumes for the different blends nearly collapse to the corresponding PVAc values and (ii) the values being closely related to the repeat unit volume of vinyl acetate, thus further supporting the notion that the observed dynamics reflect the PVAc segmental dynamics in the blends. We should note here that the $T - T_g$ scaling of the apparent activation volume does not imply the validity of the free volume model. In the majority of flexible polymers the segmental dynamics in the vicinity of T_g reflect intramolecular dynamics through the energy barriers.[50]

The glass temperature (defined at $\tau \sim 100$ s) obtained through the "isobaric" and "isothermal" experiments in the blends are compared with the bulk PVAc in Figure 9. T_g of glass-forming liquids is an increasing function of pressure. Within the free volume picture this behavior is attributed to an increase of molecular packing and the squeeze of free volume. Within models emphasizing intramolecular correlations this effect can be traced to the difficulty of conformational transitions. Different functional forms have been proposed to account for the $T_g(P)$ dependence that display usually a nonlinear character.[19] In addition, there is a decline of the gradient of the $T_g(P)$ curve on increasing pressure. These experimental features for the $T_g(P)$ dependence of bulk PVAc and for the PVAc component in the PVA-rich blends can be well captured by the following empirical equation[51]

$$T_g(P) = T_g(0)\left(1 + \frac{\kappa}{\lambda}P\right)^{1/\kappa} \tag{11}$$

where $T_g(0)$ is the value of T_g at atmospheric pressure and κ, λ are constants. These values together with the pressure

dx.doi.org/10.1021/ma301086a | Macromolecules 2012, 45, 6272−6280

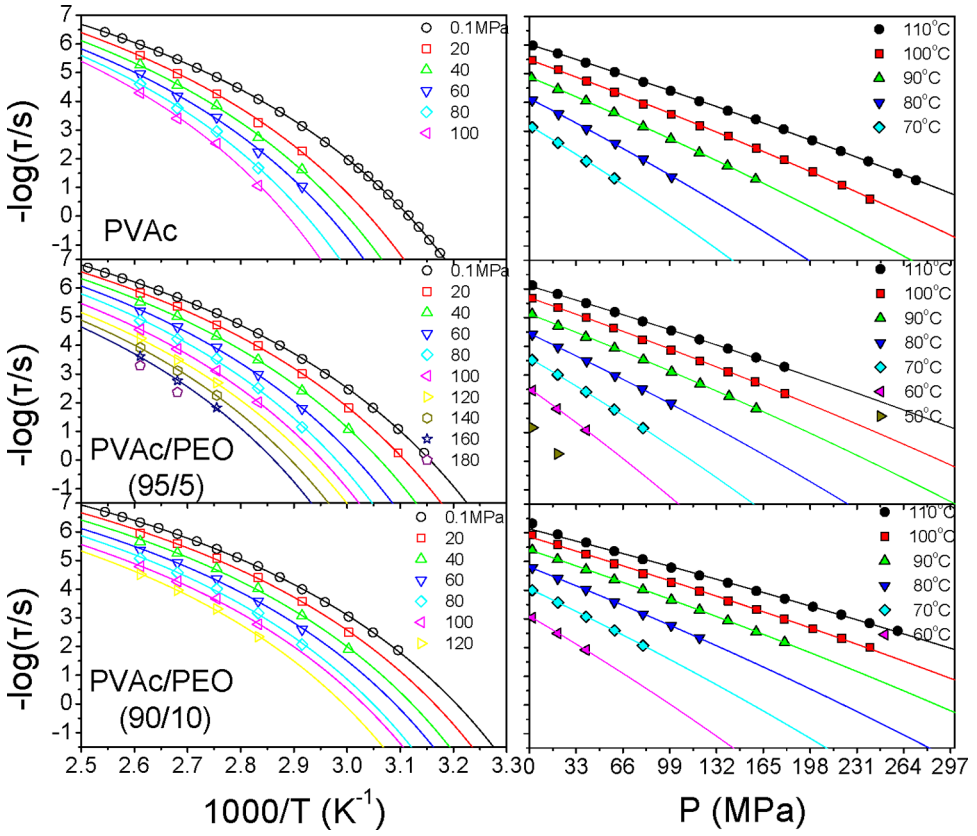

Figure 6. Segmental relaxation times for the bulk PVAc (top) and the PVAc/PEO blends with φ_{PVAc} = 0.95 (middle) and φ_{PVAc} = 0.90 (bottom) obtained from the "isobaric" (left) and "isothermal" (right) representations, respectively. Lines are fits to eqs 3 and 8, respectively.

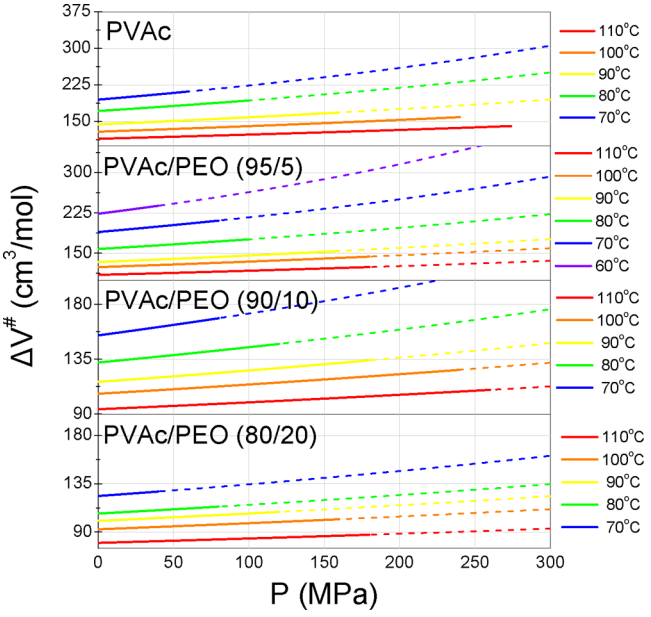

Figure 7. Apparent activation volume for the PVAc homopolymer (top) and the blends with φ_{PVAc} = 0.95 (second from top), φ_{PVAc} = 0.90 (third from top), and φ_{PVAc} = 0.80 (bottom) plotted as a function of pressure for different temperatures as indicated. The solid lines are fits according to eq 10.

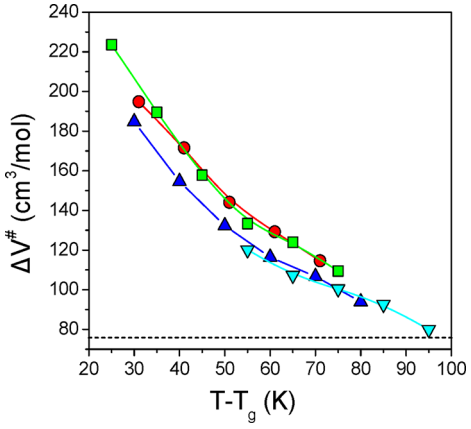

Figure 8. Apparent activation volume at 0.1 MPa as a function of the temperature difference from the respective T_g for bulk PVAc (circles) and the PVAc/PEO blends with φ_{PVAc} = 0.95 (squares), φ_{PVAc} = 0.90 (up triangles), and φ_{PVAc} = 0.80 (down triangles). Lines are guides for the eye. The dashed line gives the volume of the PVAc repeat unit.

sensitivity of T_g, $(dT_g/dP)_{P\to 0}$, are given in Table 2. Again, the $T_g(P)$ in the blends is very similar to bulk PVAc consistent with the notion as reflecting the PVAc segmental dynamics only shifted to lower temperatures.[52]

It is natural at this point to ask if the self-concentration model is capable of describing the blend dynamics at elevated pressures. This is tested in Figure 10 where the glass temperatures in bulk PVAc and in the PVAc-rich blends extracted through Figure 9 are plotted for the different pressures investigated. Evidently, the self-concentration model can only qualitatively describe the PVAc $T_g(\varphi)$ in the blends with φ_{PVAc} = 0.95, 0.90, and 0.80 within the pressure range from 0.1 to 200 MPa (no adjustable parameters).

dx.doi.org/10.1021/ma301086a | Macromolecules 2012, 45, 6272−6280

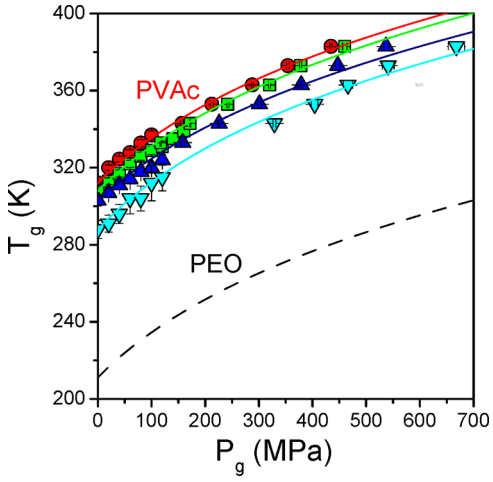

Figure 9. Pressure dependence of the glass temperature of PVAc homopolymer (circles) and of the PVA$_C$/PEO blends with φ_{PVAc} = 0.95 (squares), 0.9 (up triangles), and 0.8 (down triangles). Data are obtained from the "isothermal" and "isobaric" representations by extrapolation to τ = 100 s. The solids lines are fits to eq 11.

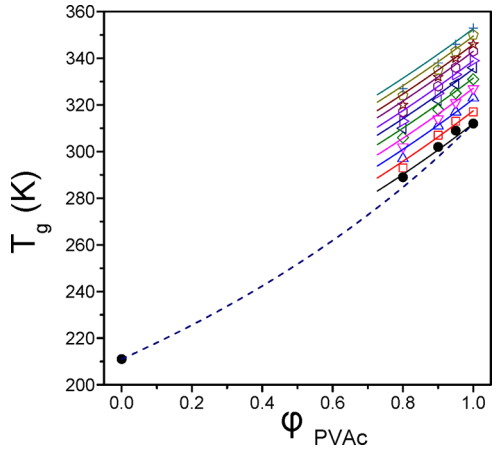

Figure 10. Glass temperatures (defined at τ = 100 s) for the PVAc homopolymer and the blends with φ_{PVAc} = 0.95, 0.9, and 0.8 plotted for different pressures: P = 0.1 MPa (spheres), 20 MPa (squares), 40 MPa (up triangles), 60 MPa (down triangles), 80 MPa (rhombi), 100 MPa (left triangles), 120 MPa (right triangles), 140 MPa (hexagon), 160 MPa (stars), 180 MPa (pentagons), and 200 MPa (crosses). Solid lines give the predictions of the LM model with φ_S = 0.22 (no adjustable parameters). The dashed line is the Fox equation at 0.1 MPa.

A more critical test of the model is by exploring its capability to predict the full $\tau(P)$ dependence under "isobaric" and "isothermal" conditions as those of Figure 6. To this end the modified VFT equation for pressure (eq 8) is employed, with parameter C fixed to the PVAc homopolymer value, and by further assuming that the ideal glass pressure varies with composition as

$$P_0(\varphi_{eff}^A) - P_g(\varphi_{eff}^A) = P_0^A - P_g^A \quad (12)$$

where P_0 is the ideal glass pressure of PVAc and $P_0(\varphi_{eff})$ is the ideal glass pressure for the slow (PVAc) component in the blend. For the composition dependence of the glass pressure we assume

$$P_g(\varphi_{eff}) = \varphi_{eff} P_g^A + (1 - \varphi_{eff}) P_g^B \quad (13)$$

in analogy to eq 6 for the $T_g(\varphi_{eff})$. Representative fits with a fixed Kuhn length to the PVAc homopolymer (l_K = 1.36 nm, φ_S = 0.22) are shown in Figure 11 for two blend compositions and for pressures in the range from 0.1 to 100 MPa. The comparison shows a qualitative agreement for all blend compositions as with the $\tau(T)$ dependence at atmospheric pressure.

In conclusion, a single characteristic length scale and a single PVAc self-concentration of $\varphi_S \sim 0.22$ qualitatively account for the segmental dynamics in thermodynamically miscible PVAc/PEO blends both at atmospheric and at elevated pressures. The much lower reported value (of 0.08) could result from phase separation at elevated temperatures and/or the use of the terminal instead of the segmental dynamics.

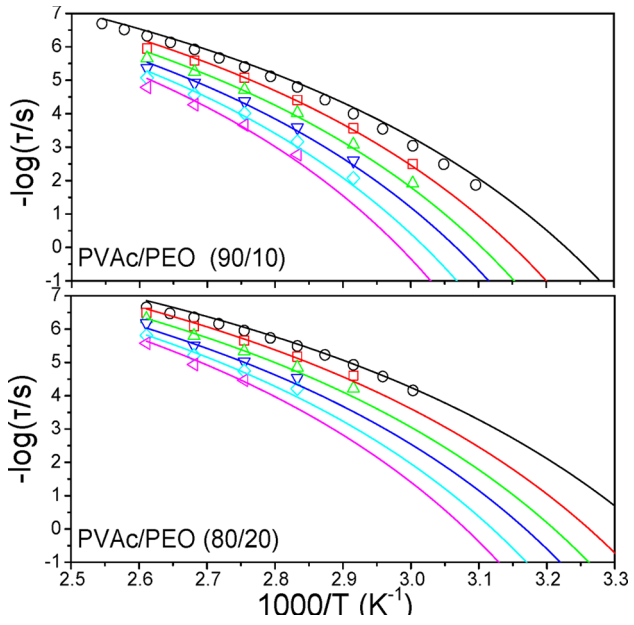

Figure 11. Segmental relaxation times for the PVAc/PEO blends with φ_{PVAc} = 0.9 (top) and φ_{PVAc} = 0.80 (bottom) at different pressures: (circles) P = 0.1 MPa, (squares) 20 MPa, (up triangles) 40 MPa, (down triangles) 60 MPa, (rhombi) 80 MPa, and (left triangles) 100 MPa. Lines give the predictions of the LM model with a fixed PVAc self-concentration of φ_S = 0.22, without any adjustable parameters.

Table 2. Parameters of the *P*-Dependence of the Glass Temperature for PVAc and the Blends (Eq 11)

	$(dT_g/dP)_{P\to 0}$	$T_g(0)$	κ	λ (MPa)
PVAc	0.29	312.1 ± 0.4	6.25 ± 0.73	1090 ± 70
PVAc/PEO (95/5)	0.22	308.6 ± 2.3	3.71 ± 0.38	1390 ± 70
PVAc/PEO (90/10)	0.20	302.7 ± 2.8	3.36 ± 0.33	1490 ± 70
PVAc/PEO (80/20)	0.24	288.0 ± 4.7	4.34 ± 0.62	1180 ± 130

dx.doi.org/10.1021/ma301086a | *Macromolecules* 2012, 45, 6272−6280

CONCLUSION

PVAc/PEO blends are thermodynamically homogeneous yet possess dynamic heterogeneity. Thermodynamic homogeneity in the PVAc-rich blends here is evidenced through X-ray scattering. In addition, all short-range correlations in the same blends were found to be dominated by PVAc. The PVAc segmental dynamics was studied as a function of composition, temperature, and pressure. An invariant frequency dispersion for the PVAc segmental dynamics in the blends at every blend composition was found when the spectra were compared under isochronal conditions. This suggests the covariance of the width of the distribution with the structural relaxation time as found in other glass-forming liquids. The self-concentration model with a PVAc self-concentration of ~0.22 can qualitatively—but not quantitatively—describe the temperature dependence of the segmental dynamics in the blends with φ_{PVAc} = 0.95 and 0.9. Similarly, the model can qualitatively account for the segmental dynamics at elevated pressures using the same self-concentration.

ASSOCIATED CONTENT

Supporting Information

Figures S1 and S2. This material is available free of charge via the Internet at http://pubs.acs.org.

AUTHOR INFORMATION

Corresponding Author

*E-mail: gfloudas@cc.uoi.gr.

Notes

The authors declare no competing financial interest.

ACKNOWLEDGMENTS

This research has been cofinanced by the European Union (European Social Fund - ESF) and Greek national funds through the Operational Program "Education and Lifelong Learning" of the National Strategic Reference Framework (NSRF) - Research Funding Program: THALIS. Investing in knowledge society through the European Social Fund.

REFERENCES

(1) Colby, R. H. *Polymer* **1989**, *30*, 1275.
(2) Roland, C. M.; Ngai, K. L. *Macromolecules* **1991**, *24*, 2261.
(3) Roovers, R. H.; Toporowski, P. M. *Macromolecules* **1992**, *25*, 1096.
(4) Chin, Y. H.; Zhang, C.; Wang, P.; Inglefield, P. T.; Jones, A. A.; Kambour, R. P.; Bendler, J. T.; White, D. M. *Macromolecules* **1992**, *25*, 3031.
(5) Pathak, J. A.; Colby, R. H.; Floudas, G.; Jerome, R. *Macromolecules* **1999**, *32*, 2553.
(6) He, Y.; Lutz, T. R.; Ediger, M. D. *J. Chem. Phys.* **2003**, *119*, 9956.
(7) Krygier, E.; Lin, G.; Mendes, J.; Mukandela, G.; Azar, D.; Jones, A. A.; Pathak, J. A.; Colby, R. H.; Kumar, S. K.; Floudas, G.; Krishnamoutri, R.; Faust, R. *Macromolecules* **2005**, *38*, 7721.
(8) Ngai, K. L.; Roland, C. M. *Rubber Chem. Technol.* **2004**, *77*, 579; *Macromolecules* **2004**, *37*, 2817.
(9) Zetsche, A.; Fischer, E. W. *Acta Polym.* **1994**, *45*, 168.
(10) Lodge, T. P.; McLeish, T. C. B. *Macromolecules* **2000**, *33*, 5278.
(11) Chung, G.-C.; Kornfield, J. A.; Smith, S. D. *Macromolecules* **1994**, *27*, 964.
(12) Kumar, S. K.; Colby, R. H.; Anastasiadis, S. H.; Fytas, G. *J. Chem. Phys.* **1996**, *105*, 3777.
(13) Kamath, S.; Colby, R. H.; Kumar, S. K.; Karatasos, K.; Floudas, G.; Fytas, G.; Roovers, J. E. L. *J. Chem. Phys.* **1999**, *111*, 6121.
(14) Shenogin, S.; Kant, R.; Colby, R. H.; Kumar, S. K. *Macromolecules* **2007**, *40*, 5767.
(15) Kant, R.; Kumar, S. K.; Colby, R. H. *Macromolecules* **2003**, *36*, 10087.
(16) Cangialosi, D.; Alegria, A.; Colmenero, J. *Macromolecules* **2006**, *39*, 7149.
(17) Colby, R. H.; Lipson, J. E. G. *Macromolecules* **2005**, *38*, 4919.
(18) Lipson, J. E. G.; Milner, S. T. *J. Polym. Sci., Polym. Phys.* **2006**, *44*, 3528.
(19) Floudas, G.; Paluch, M.; Grzybowski, A.; Ngai, K. L. *Molecular Dynamics of Glass-Forming Systems. Effects of Pressure*; Springer: Berlin, 2011.
(20) Floudas, G. *Prog. Polym. Sci.* **2004**, *29*, 1143.
(21) Floudas, G.; Fytas, G.; Reisinger, T.; Wegner, G. *J. Chem. Phys.* **1999**, *111*, 9129.
(22) Zhang, S. H.; Casalini, R.; Runt, J.; Roland, C. M. *Macromolecules* **2003**, *36*, 9917.
(23) Mpoukouvalas, K.; Floudas, G.; Verdock, B.; Du Prez, F. E. *Phys. Rev. E* **2005**, *72*, 011802.
(24) Mpoukouvalas, K.; Floudas, G.; Zhang, S. H.; Runt, J. *Macromolecules* **2005**, *38*, 552.
(25) Schwartz, G. A.; Colmenero, J.; Alegria, A. *Macromolecules* **2007**, *40*, 3246.
(26) Roland, C. M.; Casalini, R. *Macromolecules* **2007**, *40*, 3631.
(27) Gitsas, A.; Floudas, G.; White, R. P.; Lipson, J. E. G. *Macromolecules* **2009**, *42*, 5709.
(28) Gitsas, A.; Floudas, G.; Butt, H.-J.; Pakula, T.; Matyjaszewski, K. *Macromolecules* **2010**, *43*, 2453.
(29) Mpoukouvalas, K.; Floudas, G. *Macromolecules* **2008**, *41*, 1552.
(30) Yin, Z.; Y.; Alfonso, G. C.; Turturro, A.; Pedemonte, E. *Polymer* **1993**, *34*, 1465.
(31) Chen, X.; An, L.; Li, L.; Yin, J.; Sun, Z. *Macromolecules* **1999**, *32*, 5905.
(32) Silvestre, C.; Karasz, F. E.; MacKnight, W. J.; Martuscelli, E. *Eur. Polym. J.* **1987**, *10*, 745.
(33) Fragiadakis, D.; Runt, J. *Macromolecules* **2010**, *43*, 1028.
(34) Urakawa, O.; Ujii, T.; Adachi, K. *J. Non-Cryst. Solids* **2006**, *352*, 5042.
(35) Zhao, J.; Zhang, L.; Ediger, M. D. *Macromolecules* **2008**, *41*, 8030.
(36) Tyagi, M.; Arbe, A.; Colmenero, J.; Frick, B.; Stewart, J. R. *Macromolecules* **2006**, *39*, 3007.
(37) Tyagi, M.; Arbe, A.; Alegria, A.; Colmenero, J.; Frick, B. *Macromolecules* **2007**, *40*, 4568.
(38) Havriliak, S.; Negami, S. *Polymer* **1967**, *8*, 161.
(39) Floudas, G. Dielectric Spectroscopy. In *Polymer Science: A Comprehensive Reference*; Matyjaszewski, K., Möller, M., Eds.; Elsevier BV: Amsterdam, 2012; Vol. 2.32, pp 825−845.
(40) Guinier, A. *X-ray Diffraction in Crystals, Imperfect Crystals and Amorphous Bodies*; W.H. Freeman: San Francisco, 1963.
(41) MacGlashan, G. S.; Andreev, Y. G.; Bruce, P. G. *Nature* **1999**, *398*, 792.
(42) Roland, C. M.; Casalini, R. *Macromolecules* **2003**, *36*, 1361.
(43) Wu, S. *J. Polym. Sci., Polym. Phys. Ed.* **1989**, *27*, 723.
(44) Fetters, L. J.; Lohse, D. J.; Richter, D.; Witten, T. A.; Zirkel, A. *Macromolecules* **1994**, *27*, 4639.
(45) Roland, C. M.; Casalini, R.; Paluch, M. *Chem. Phys. Lett.* **2003**, *367*, 259.
(46) Ngai, K. L. *J. Non-Cryst. Solids* **2005**, *351*, 2635; *J. Phys.: Condens. Mater.* **2003**, *15*, S1107. *Relaxation and Diffusion in Complex Systems*; Springer: New York, 2011.
(47) Paluch, M.; Patkowski, A.; Fischer, E. W. *Phys. Rev. Lett.* **2000**, *85*, 2140.
(48) Floudas, G.; Gravalides, C.; Reisinger, T.; Wegner, G. *J. Chem. Phys.* **1999**, *111*, 9847.
(49) Floudas, G.; Reisinger, T. *J. Chem. Phys.* **1999**, *111*, 5201.
(50) Floudas, G.; Mpoukouvalas, K.; Papadopoulos, P. *J. Chem. Phys.* **2006**, *124*, 074905.
(51) Andersson, S.; Andersson, O. *Macromolecules* **1998**, *31*, 2999.

(52) The crystallization of PEO precludes an investigation of its $T_g(P)$. Herein we have assumed either (i) the same dependence as for PVAc or as an alternative (ii) the same dependence as the pressure dependence of its melting temperature, without substantial difference.